Drone-Based Photogrammetry for Pavement Deterioration Detection and Quantification in Airport Infrastructure

Guido Staub [1], Elisabet Jara [1],

[1] University of Concepción, Department for Geodetic Sciences and Geomatics, Los Ángeles, Chile – gstaub@udec.cl, ejara2019@udec.cl

Keywords: Drone Photogrammetry, Airport Infrastructure, Pavement Deterioration, Image Processing

Abstract

The maintenance of airport pavements is critical to ensuring the safety and efficiency of air operations. Conventional inspection methods are often time-consuming, subjective, and prone to inconsistencies in data collection. Recent advances in unmanned aerial vehicle (UAV) photogrammetry offer a potential alternative for improving inspection efficiency and measurement accuracy. This study evaluates the applicability of UAV-based photogrammetry for the detection and quantification of pavement distresses under conditions representative of airport infrastructure. Image data were acquired at different flight altitudes and overlap configurations and processed using Structure-from-Motion techniques to generate high-resolution orthomosaics and Digital Elevation Models (DEMs). The resulting datasets were analyzed to identify, delineate, and classify deterioration types and severity levels. The results indicate that a flight altitude of 10 m combined with 80% longitudinal and 70% transversal overlap provides an optimal balance between spatial resolution and operational efficiency. Under unobstructed conditions, photogrammetric analysis detected more than 98% of existing distresses and enabled more precise geometric delineation compared to traditional field-based methods. Undetected distresses were primarily associated with shadowed or obstructed areas, highlighting the influence of environmental conditions on detection performance. Overall, the findings demonstrate that UAV-based photogrammetry is a reliable and efficient approach for pavement condition assessment, with significant potential to enhance data quality and reduce inspection time in airport infrastructure management.

1. Introduction

Chile has over 450 airport facilities, including 344 aerodromes, 102 heliports, and 7 airports, distributed across a wide and geographically diverse territory (DGAC, 2025). Ensuring the operational safety of these infrastructures requires systematic inspection of pavement conditions, as surface deterioration can directly affect aircraft operations during landing, take-off, and taxiing. Common hazards include pavement defects, foreign object debris, drainage issues, and obstructions, all of which must be regularly monitored to maintain safety standards (Horonjeff et al., 2010; ICAO, 2025).

Traditionally, airport inspections have relied heavily on visual ground surveys conducted by trained personnel. These inspections involve the systematic evaluation of movement areas (runways, taxiways, and aprons), as well as associated elements such as lighting systems, markings, signage, safety areas, and the surrounding environment (Shah and Ahmed, 2013). Inspectors typically use standardized checklists and professional judgment to identify discrepancies and potential hazards, such as those summarized in Table 1. These inspections are often performed on a daily basis and may include nighttime evaluations to assess lighting systems, ensuring consistency and operational safety (Humphreys and Graham, 2000).

In recent years, airport inspection practices have increasingly incorporated advanced technologies to improve efficiency, accuracy, and data availability. These developments include UAV-based imaging, automated pavement assessment systems, embedded sensor networks (Xu et al., 2020), and GIS-based integration for spatial analysis and maintenance planning (Ravi et al., 2020; Yu et al., 2018; Liu et al., 2018, Ishtiaq and Siddiqui, 2017). To streamline these workflows, digital applications have been developed to manage both airside and landside inspections (Putra et al., 2024), while multi-static Ground-Penetrating Radar systems now allow for high-resolution subsurface evaluations (Yi et al., 2018). Among these approaches, UAVs have gained particular attention due to their ability to rapidly capture detailed imagery over large areas. When combined with Structure-from-Motion (SfM) photogrammetry, UAV data can be used to generate high-resolution orthomosaics and digital elevation models suitable for detailed surface analysis (Černý et al., 2022; Pamula et al., 2025). Furthermore, research has demonstrated the feasibility of using these UAV-derived models to calculate standardized metrics such as the International Roughness Index (IRI) (Cruz Toribio, 2022).

Hazard type	Description
Pavement defects	Cracks, spalling, potholes, uneven surfaces
Foreign Object Debris	Any loose objects that could damage aircraft
Marking and signage issues	Faded, incorrect, or missing markings and signs
Lighting malfunction	Burnt-out or misaligned lights
Obstructions	Objects infringing on safety areas or approach/departure paths
Drainage problems	Water accumulation on surfaces
Vegetation overgrowth	Obstructing visibility or safety areas

Table 1. Common hazard types (Horonjeff et al., 2019)

Despite these advances, most existing studies focus on the development of individual technologies or isolated applications, with limited emphasis on systematic, quantitative comparisons between UAV-based photogrammetry and standardized PCI field inspections under realistic operational conditions**.** This limitation

is particularly relevant in airport environments, where strict safety requirements, operational constraints, and large pavement areas demand both high accuracy and rapid data acquisition.

In Chile, the Pavement Condition Index (PCI) is currently employed as a standard tool for assessing pavement condition and supporting maintenance planning (Prado et al., 2024). PCI surveys are typically conducted on an annual or biennial basis, depending on operational conditions. However, in practice, PCI data are not always available within the required timeframes due to the labor-intensive nature of field surveys, operational constraints, and environmental factors. This can result in temporal gaps between data acquisition and decision-making, potentially affecting the effectiveness of maintenance strategies. Additionally, traditional inspection methods rely on manual measurements and visual assessments, which may introduce subjectivity and limit measurement precision, particularly for irregular or spatially extensive distresses (FAA, 2014).
In this context, UAV-based photogrammetry emerges as a promising alternative, offering rapid data acquisition and high-resolution surface representation. However, its effectiveness for standardized pavement condition assessment, particularly in comparison with PCI-based methods, remains insufficiently quantified.
To address this gap, this study investigates the feasibility of using UAV-based photogrammetry for the detection and quantification of pavement distresses in both rigid and flexible pavements. The main contributions of this work are:

- a **quantitative comparison** between UAV-based photogrammetric analysis and traditional PCI-based field inspections;
- an **evaluation of acquisition parameters** (flight altitude and image overlap) in relation to distress detectability;
- an **assessment of operational efficiency gains** in terms of data acquisition time; and
- an analysis of **limitations related to environmental conditions**, such as shadows and obstructions, including potential mitigation strategies.

The results demonstrate detection rates exceeding 98% under unobstructed conditions, highlighting the strong potential of UAV-based approaches for improving the efficiency and reliability of airport pavement inspections. By addressing both methodological and operational aspects, this work aims to support the integration of UAV-based approaches into airport pavement management systems.

2. Methodology

2.1 Sample Site Selection

The selection of study sites focused on areas representative of airport pavement conditions, including both rigid (concrete) and flexible (asphalt) surfaces. Priority was given to unobstructed locations suitable for UAV operations, exhibiting a variety of deterioration types and severity levels. This enabled a direct comparison between traditional field measurements and photogrammetric analysis.

Due to operational constraints in active airport environments, analogous surfaces with similar geometric and material characteristics were selected, including multi-sport courts and open-air parking areas. From an initial set of four candidate sites, two were selected based on the presence of visible deterioration, minimal obstructions, and authorization for data acquisition. The selected sites included a concrete pavement area of approximately 600 m² and an asphalt pavement area of approximately 800 m².

Although these sites do not represent active airport environments, their surface characteristics and deterioration patterns are comparable to airfield pavements, allowing controlled evaluation of the proposed methodology.

2.2 Data Acquisition and Flight Planning

A DJI Phantom 4 Pro UAV equipped with a 1-inch CMOS RGB sensor was used for image acquisition. The sensor has a focal length of 8.8 mm and captures images with a resolution of 5472 × 3648 pixels (DJI, 2017). Flight planning was designed to evaluate the influence of acquisition parameters on data quality and distress detectability.

Two flight altitudes (10 m and 15 m) were selected to balance spatial resolution and operational efficiency. The corresponding Ground Sample Distance (GSD) was calculated as approximately 5 mm/px at 10 m and 7.5 mm/px at 15 m. These values were selected considering that low-severity distresses, such as fine cracks, typically exhibit widths on the order of a few millimeters, requiring sufficiently high spatial resolution for reliable detection.

Three image overlap configurations were tested: 70%/60%, 80%/70%, and 90%/80% (longitudinal/transversal). These configurations were evaluated in terms of image alignment quality, model completeness, number of images, and processing requirements.

Environmental conditions were considered during flight planning, as illumination and occlusions directly influence image quality. Flights were conducted under stable meteorological conditions (wind speeds < 10 m/s and consistent illumination), although shadow effects and temporary obstructions (e.g., parked vehicles) could not be fully controlled and were later analyzed as part of the methodological limitations.

To improve georeferencing accuracy, Ground Control Points (GCPs) were used. Three GCPs were distributed across each study site, ensuring spatial coverage across the corners and central regions of the study area. One GCP was measured in static GNSS mode and connected to the Continuously Operating Reference Station (CORS) UDEC00CHL, while the remaining points were measured in rapid-static mode. The expected positioning accuracy of the GCPs was within the centimeter range.

2.3 Photogrammetric Processing

Image processing was performed following a standard Structure-from-Motion (SfM) workflow using photogrammetric software (e.g., Agisoft Metashape). The workflow included image alignment, sparse point cloud generation, GCP-based georeferencing, camera optimization, dense point cloud generation, and derivation of orthomosaics and Digital Elevation Models (DEMs).

To ensure data quality and geometric reliability, several accuracy metrics were evaluated:

- **Reprojection error:** used to assess the internal consistency of the photogrammetric model;

- **Ground Control Point residuals:** used to evaluate georeferencing accuracy;
- **Root Mean Square Error (RMSE):** calculated for horizontal and vertical components based on GCP residuals.

The final models achieved horizontal RMSE values in the sub-centimeter to centimeter range and vertical RMSE values in the centimeter range, depending on flight configuration and image quality. Lower flight altitudes and higher overlap percentages generally resulted in improved geometric accuracy and model completeness.

2.4 Deterioration Detection and Quantification

Deterioration assessment was conducted using both traditional field methods and photogrammetric analysis to enable a direct and consistent comparison between approaches. A simplified reference guide, developed for this study and based on established manuals (Shahin, 2005), was used to standardize the identification, classification, and severity assessment of distress types for both rigid and flexible pavements.
To ensure comparability, both methods followed the same classification criteria and measurement units as defined in the Pavement Condition Index (PCI) methodology. Distresses were categorized by type and severity level (low, medium, high), based on geometric and visual characteristics such as crack width, extent of material loss, and surface deformation.

For photogrammetric analysis, orthomosaics and Digital Elevation Models (DEMs) were examined at multiple scales to ensure accurate identification and delineation of distresses.
In concrete pavements, the analysis began with the delineation of individual slabs using the orthomosaic to define discrete evaluation units. Each slab was systematically inspected at a scale of approximately 1:25, following a structured path from edges and joints toward the center to ensure complete coverage. When a deterioration was identified, it was digitized at a finer scale (approximately 1:10) using polylines or polygons, depending on its geometry. Severity levels were assigned according to predefined criteria, considering parameters such as crack width, degree of spalling, and slab fragmentation.
To complement the visual analysis, DEMs were used to assess depth-related distresses. Elevation profiles were extracted along selected transects across identified deteriorations, allowing the quantification of vertical deviations and supporting severity classification, particularly for distresses such as depressions or faulting.

In asphalt pavements, the analysis was conducted continuously across the orthomosaic, as no predefined slab structure exists. The inspection followed a systematic spatial progression to ensure full surface coverage. When a deterioration was identified, it was classified and delineated using polylines for linear distresses (e.g., cracks) and polygons for areal distresses (e.g., rutting, patching). Measurements were obtained directly from the digitized geometries, allowing precise calculation of lengths and areas. DEM analysis was similarly used to quantify depth-related distresses, with particular attention to rutting, where profiles were extracted perpendicular to the direction of traffic to account for cross slopes.
Traditional field measurements were conducted following standard PCI procedures. Distresses were identified visually, measured using instruments such as measuring tapes and odometers, and recorded on inspection forms. These forms included sketches indicating the approximate spatial distribution of distresses, along with quantitative measurements and severity classifications. To ensure consistency with the photogrammetric analysis, customized forms were developed for each study site, incorporating identifiable surface features to improve spatial referencing.
For the comparative analysis, distresses detected by both methods were matched based on spatial location and type. Differences in detection, measurement (length or area), and severity classification were recorded and analyzed. Particular attention was given to discrepancies arising from methodological differences, such as the simplification of crack geometry in field measurements or visibility limitations in photogrammetric data.
This matching process enabled the quantification of detection rates, measurement deviations, and agreement in severity classification between both methods.

2.5 Methodological Limitations and Mitigation Strategies

Several factors affecting detection performance were identified during data acquisition and analysis. Shadows and occlusions were found to significantly impact the visibility of low-severity distresses, particularly in concrete pavements. Additionally, parked vehicles prevented complete surface observation in some areas.
To mitigate these effects, several strategies are recommended:

- scheduling flights near solar noon to minimize shadow length;
- conducting multi-temporal acquisitions to reduce persistent occlusions;
- using high dynamic range (HDR) imaging to improve visibility in high-contrast conditions;
- incorporating additional sensors (e.g., multispectral or thermal) to enhance detection capabilities;
- ensuring operational coordination to minimize surface obstructions during data acquisition.

These considerations are essential for improving the robustness, reliability, and operational applicability of UAV-based pavement inspection workflows.

3. Results

For both asphalt and concrete pavements, certain distresses at low and medium severity levels require measurements with a certain GSD due to their geometric characteristics. This implies that some distresses were not clearly discernible at a 15m flight altitude, as the pixel size exceeded the width of these deteriorations. While distresses might be visible at both 10 m and 15 m altitudes, the challenge lies in accurately delineating them, measuring their dimensions, and determining their severity level. The resolution attained at these altitudes did not allow for capturing the finer irregularities of the pavement in detail (Figure 1).

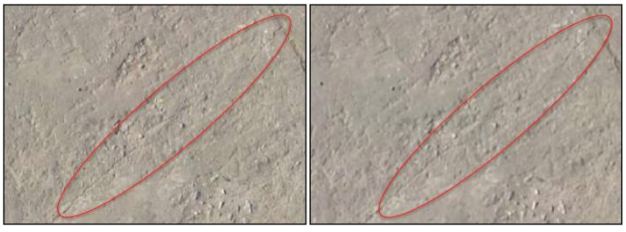

Figure 1. Observation of the same deterioration at flight heights of 10m (left) and 15m (right)

Furthermore, different combinations of longitudinal and transverse overlaps were evaluated, considering parameters such as the number of captured photographs, memory usage, and the

quality of the generated orthomosaics and DEMs. A considerable increase in the number of photographs and required storage was observed with increasing overlap percentages. Regarding the quality of the orthomosaics, no significant differences were noted between the 80%-70% and 90%-80% overlap combinations. However, the 70%-60% combination exhibited minor deficiencies in image alignment, as illustrated in Figure 2, which shows imperfections and irregularities at the edge of the central object.

Figure 2. Comparison of a specific area within orthomosaics derived from different overlap combinations (left:70%-60%; centre: 80%-70%; right: 90%-80%)

In concrete pavements, distresses were measured per slab. Across a total of 27 evaluated slabs, 8 of the 15 classified distress types for this pavement type were identified. Using the traditional field survey method, 97 distresses were measured, while photogrammetric analysis recorded 93 distresses. Of these, 81 distresses were detected by both methods, with 80 exhibiting the same severity level; 16 distresses were identified solely through traditional field measurement; 12 distresses were measured only via photogrammetric analysis; A total of 109 distresses were present at the site.

The slabs where the 16 distresses detected solely in the field were located were examined. It was observed that 4 of these corresponded to slabs with vehicles parked on them at the time of the flights. Due to this obstruction, only visible areas could be evaluated, preventing the recording of distresses under the vehicles, which affected complete detection. Of the remaining 12 distresses recorded only by the traditional field method, 11 were identified on slabs fully or partially covered by shadows, either from adjacent infrastructure or nearby trees. These distresses included: 2 cases of corner spalling at a low severity level, 3 cases of transverse and longitudinal joint spalling at a low severity level, 3 instances of raveling, 1 case of map cracking at a low severity level, and 2 contraction cracks. This indicates that the presence of shadows hinders the detection of these types of distresses at low severity levels.

The remaining distress, not found on a slab with obstruction or covered by shadow, corresponded to a case where three distresses of the same type were recorded for that slab, although only two were drawn on the sketch. This suggests a potential issue arising from the manual field data collection system, indicating a recording error during the inspection.

Of the 12 distresses detected solely through photogrammetric analysis, 7 were map cracking, 3 were raveling, and 2 were transverse and longitudinal joint spalling. This indicates that map cracking and raveling are identified more accurately through photogrammetric analysis, as they are evaluated across the entire slab, making their field evaluation more complex and susceptible to omission in the record.

An analysis was conducted on the single distress recorded by both methods with different severity levels. This corresponded to map cracking. The traditional field measurement recorded only a medium severity level, while photogrammetric analysis identified both low and medium severity levels. Although the PCI method typically records only the highest severity level for a single distress, this study opted to record all observed severity levels on each slab for a more detailed analysis.

All the above-mentioned results in case of concrete pavement are summarized in table 2.

Deterioration	Percentage	
Detected by both methods	74,3	Relative to the total deteriorations at the site (109)
Detected by traditional method	89	
Detected by photogrammetric analysis	85,3	
Detected with Photogrammetric Analysis on unobstructed slabs	99,1	
With matching severity level	98,8	Relative to the total deteriorations detected by both methods (81)

Table 2. Detection and correspondence percentages of deteriorations by evaluation method on concrete pavement

In asphalt pavements, distresses are measured in linear meters or square meters, depending on the distress type. At the study site, 8 of the 16 classified distress types for this pavement type were identified. Using the traditional field survey method, a total of 57 distresses were recorded, while photogrammetric analysis recorded 68 distresses. Of these, 56 distresses were detected by both methods, with 51 exhibiting the same severity level; 1 distress was identified solely through traditional field measurement; 12 distresses were measured only via photogrammetric analysis; A total of 69 distresses were present at the site.

Of the distresses found by both methods, 37 corresponded to linear cracking, which is measured in linear meters. Comparing the measurements of these distresses revealed that 8 showed no differences. 15 distresses had differences ranging from 0.1 m to 0.2 m: This can be attributed to the field measurement method, where an odometer is used to attempt to follow the crack's shape. However, this procedure does not accurately capture the entire sinuous form of the crack. Conversely, measurements made via photogrammetric analysis allow for following the actual shape of the distress, reducing variations in the final result. 6 distresses had differences between 0.3 m and 0.4 m: In 2 of these cases, the differences can again be attributed to the field measurement method compared to photogrammetric analysis. One distress exceeded 10 m in length, which can lead to accumulated differences when measuring with an odometer, while the other distress had an irregular crack shape, making precise field measurement difficult. For the remaining 4 distresses, the differences may be due to this same situation or a limitation in the visibility of the cracks in the orthomosaic. The remaining 8 distresses showed larger discrepancies, with differences ranging from 0.5 m to 1.5 m. These discrepancies are related to the delineation method for distresses measured in square meters. In the traditional field method, these distresses are delineated using a rectangle that covers the entire distress or most of it, leading to inaccuracies by not precisely following the actual edges of the deterioration. This delineation method causes significant differences in distress measurements.

Of the remaining 19 distresses, all corresponded to types of distresses measured in square meters. Among these, 3 were cases of fatigue cracking, which showed measurement differences of up to 1.5 sqm; 6 corresponded to block cracking, where 4 had area differences between 0.6 sqm and 1.1 sqm, while the other 2

cases showed more significant differences, reaching areas of 5.2 sqm and 9.3 sqm. 2 distresses were depressions, with minor differences between the methods, recording discrepancies of 0 and 0.4 sqm. 1 distress was caused by fuel spillage and showed no differences between the measurement methods. 1 corresponded to patching, which also showed no differences in measurements. 3 distresses were aggregate loss and scaling, where differences between 3.1 sqm and 5.5 sqm were observed, with higher values in the traditional field measurement. 3 corresponded to rutting, recording significant differences between both methods, reaching discrepancies of up to 11.3 sqm, with higher measurements obtained through photogrammetric analysis.
All the above-mentioned results in case of asphalt pavement are summarized in table 3.

Deterioration	Percentage	
Detected by both methods	81,2	Relative to the total deteriorations at the site (69)
Detected by traditional method	82,6	
Detected by photogrammetric analysis	98,6	
With matching severity level	91,1	Relative to the total deteriorations detected by both methods (56)

Table 3. Detection and correspondence percentages of deteriorations by evaluation method on asphalt pavement

PCI measurement in airport infrastructure can take from several weeks to months, depending on various factors. These include the total area to be evaluated, the pavement condition, the experience of the evaluators, weather conditions, and the number of operations scheduled during the measurement dates, which can affect work continuity. During the time it takes to complete these measurements, new distresses may develop due to continuous aircraft traffic or environmental conditions, or existing distresses may evolve, increasing their severity. This highlights the importance of performing measurements efficiently to obtain accurate and representative data on the actual pavement condition. In this study, for the same pavement area, the time required with the traditional method was approximately 3 hours, while the flight time was only 5.5 minutes. Although the additional time required for control point acquisition should be considered, this can be performed concurrently with the flights. Accordingly, this method could represent a significant improvement in reducing operational disruption times at airport infrastructures.
Figure 3 and 4 show the location sketches depicting the damages detected using both the traditional field measurement method and the photogrammetric analysis, allowing for a visual comparison of the results.

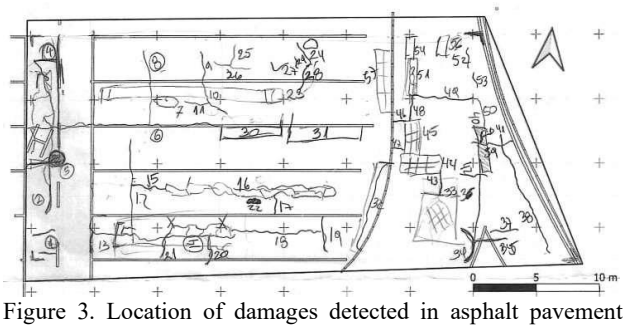

Figure 3. Location of damages detected in asphalt pavement using traditional field measurement

4. Discussion

The results demonstrate that UAV-based photogrammetry is a highly effective tool for pavement distress detection, achieving detection rates above 98% under unobstructed conditions for both concrete and asphalt pavements. These findings confirm its strong potential as an alternative to traditional PCI-based field inspections, particularly in operational environments where time efficiency is critical.

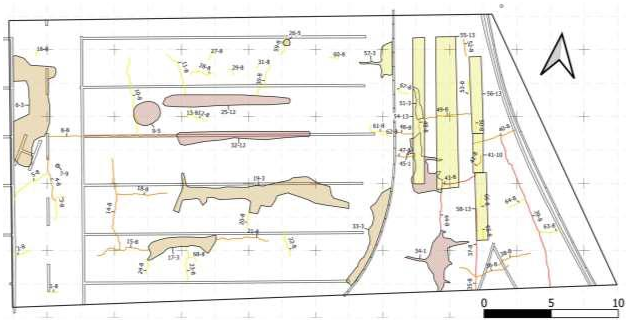

Figure 4. Location of damages detected in asphalt pavement using photogrammetric analysis

4.1 Detection performance and measurement differences

Photogrammetric analysis showed superior performance in identifying certain distress types, particularly map cracking, raveling, and rutting. These distresses are typically distributed over larger areas or exhibit irregular geometries, making them difficult to quantify accurately using conventional field methods. In contrast, UAV-derived orthomosaics allow continuous surface observation and precise delineation, reducing subjectivity and improving measurement consistency.

For linear distresses, differences between methods were primarily associated with measurement techniques. Field measurements using odometers tend to simplify the geometry of cracks, leading to systematic underestimation of their length. Photogrammetric analysis, by contrast, enables accurate tracing of sinuous crack patterns, resulting in more representative measurements.

4.2 Influence of environmental conditions

A key limitation identified in this study is the impact of environmental conditions on detection performance. Shadows and obstructions significantly affected the visibility of low-severity distresses, particularly in concrete pavements. Specifically, 11 distresses were not detected due to shadow coverage, while 4 were obscured by parked vehicles.

These findings highlight the importance of integrating **environmental considerations into the data acquisition strategy**. Several mitigation approaches can be proposed:

- **Optimal flight scheduling:** Conducting flights near solar noon reduces shadow length and improves illumination consistency.
- **Multi-temporal acquisition:** Repeating flights at different times of day can minimize persistent shadow effects.
- **High dynamic range (HDR) imaging:** Enhances detail visibility in high-contrast areas.

- **Alternative sensors:** Multispectral or thermal cameras may improve detection in shaded or low-contrast conditions.
- **Operational coordination:** Ensuring unobstructed surfaces (e.g., restricting parking during flights) can significantly improve detection completeness.

Incorporating these strategies into the methodology can enhance the robustness and reliability of UAV-based inspections.

4.3 Operational implications

One of the most significant advantages of UAV-based photogrammetry is the substantial reduction in data acquisition time. In this study, field measurements required approximately 3 hours, while UAV data acquisition was completed in 5.5 minutes. This represents a reduction of over 95% in acquisition time, with important implications for airport operations.

Shorter inspection times reduce disruption to air traffic, increase flexibility in scheduling, and enable more frequent monitoring. Additionally, the ability to perform detailed analysis in an office environment allows for data verification, repeatability, and long-term documentation, which are difficult to achieve with purely field-based methods.

4.4 Limitations and future work

Despite its advantages, this study presents several limitations. The analysis was conducted on a limited number of test sites, which, although representative, do not fully capture the variability of airport pavement conditions. Additionally, the study sites were not active runways, and therefore do not fully reflect operational constraints such as aircraft traffic or regulatory restrictions.

From a technical perspective, further validation of the geometric accuracy of orthomosaics and DEMs is required, including rigorous statistical assessment of horizontal and vertical errors. Moreover, detection performance should be evaluated across a wider range of distress types and severity levels.

Future research should also explore the integration of automated or semi-automated distress detection algorithms, which could further enhance efficiency and reduce manual interpretation efforts.

5. Conclusions

Drone-based photogrammetry has demonstrated strong potential for the identification and quantification of pavement distresses in both rigid and flexible surfaces. The results show high levels of agreement with traditional PCI-based field inspections, achieving detection rates exceeding 98% under unobstructed conditions and consistent severity classification for the majority of commonly observed distress types.

A key advantage of the proposed approach lies in its operational efficiency. Data acquisition times were significantly reduced compared to traditional methods (on the order of minutes versus hours), while enabling the generation of high-resolution, spatially continuous datasets that support detailed and repeatable analysis in an office environment. This represents a substantial improvement in terms of both inspection speed and data traceability.

The findings also indicate that photogrammetric analysis enhances the detection and measurement of certain distress types, particularly those with irregular geometries such as raveling, map cracking, and rutting. In contrast, discrepancies observed in the identification of aggregate loss and scaling suggest that detection performance may vary depending on distress characteristics and severity levels, requiring further investigation.

Environmental factors were identified as a key limitation. Shadows and occlusions, including those caused by nearby infrastructure and parked vehicles, significantly affected the visibility of low-severity distresses. These effects highlight the importance of optimized flight planning and the potential integration of complementary sensing approaches, such as high dynamic range (HDR) imaging or multispectral and thermal sensors, to improve robustness under varying conditions.

Overall, UAV-based photogrammetry provides a reliable and efficient alternative to conventional pavement inspection methods, with clear advantages in data completeness, measurement precision, and operational flexibility. Its integration into airport pavement management systems has the potential to enhance maintenance planning by providing more timely and comprehensive information on pavement condition.

Future research should focus on validating these findings across a broader range of pavement conditions, distress types, and environmental scenarios. In addition, further statistical evaluation of orthomosaic and Digital Elevation Model accuracy is required to strengthen confidence in the geometric reliability of photogrammetric products and support their adoption in operational contexts.

References

Černý, M., Tlučhoř, T., Hamza, M., 2022. Methodology for Inspecting the Correctness of the Function of Airport Lighting Systems Using a Commercially Available UAS. *New Trends in Aviation Development (NTAD)*, Novy Smokovec, Slovakia, pp. 32-36

Cruz Toribio, J. O., 2022. Cálculo del Índice de Regularidad Internacional (IRI) a través de imágenes obtenidas de un vehículo aéreo no tripulado. Universidad de Costa Rica, Sistema de Estudios de Posgrado, Maestría Académica en Ingeniería de Transporte y Vías.

DGAC, 2025. Red aeroportuaria. https://www.dgac.gob.cl/aeropuertos/red-aeroportuaria-nacional/red-aeroportuaria/. Last accessed 21.05.2025

DJI, 2017. Phantom 4 Pro / Pro+: Manual del Usuario (Ed. 1.2).https://dl.djicdn.com/downloads/phantom_4_pro/20170719/Phantom_4_Pro_Pro_Plus_User_Manual_ES.pdf.Last accessed 03.08.2024.

FAA, 2014. Advisory Circular 150/5380-6C. https://www.faa.gov/documentLibrary/media/Advisory_Circular/150-5380-6C.pdf. Last accessed 04.05.2025.

Horonjeff, R., McKelvey, F., Sproule, W., Young, S., 2010. *Planning and Design of Airports*. 5th ed. New York: McGraw-Hill Education.

Humphreys, I., Graham, F., 2000. Traditional Airport Performance Indicators: A Critical Perspective. *Transportation Research Record*. 1703. 24-30. 10.3141/1703-04.

ICAO, 2025. Airport Services Manual – Part IX – Airport maintenance practices (Doc 9137P9). https://store.icao.int/en/airport-services-manual-airport-

maintenance-practices-doc-9137-part-9. Last accessed 12.05.2025.

Ishtiaq, M., Siddiqui, M. A., 2017. Development of an Airport Pavement Management System using GIS. *International Journal of Engineering Research & Technology (IJERT)*, 6(11), 312-316

Liu, M., Sun, L., Fan, X., 2018. A Review of Smart Pavement Technologies for Structural Health Monitoring. Journal of Traffic and Transportation Engineering (English Edition), 5(4), 285-299.

Pamuła, W., Pamuła, T., Stenzel, T., Sajkowski, M., Rytter, A., Żuchowska, D., 2025. UAV-Based Airport Lights Inspection Without GNSS Positioning Support. *Remote Sensing*, *17*(6), 1013.

Prado, Q., Advias, C., Durand, M., Tedy. J., 2023. Evaluación superficial del pavimento asfáltico apoyada por el método PCI en pistas de aterrizaje de aeropuertos. *Universidad, Ciencia y Tecnología*, *27*(118), 87-98.

Putra, J., Winiasri, L., Rozi, F., Moonlight, L., 2024. Development of Airport Airside and Landside Facilities Inspection Application: Enhancing Safety and Efficiency. *Appissode: Application, Information System and Software Development Journal*, *2*(3), 1-9

Ravi, R., Bullock, D., Habib, A., 2020. Highway and airport runway pavement inspection using mobile LiDAR. *Int. Arch. Photogramm. Remote Sens. Spatial Inf. Sci*., XLIII-B1-2020, 349–354

Shah, Y. K., Ahmed, K., 2013. Review of Airport Pavement Maintenance Practices in Developing Countries. *Journal of Transportation Engineering*, 139(2), 178-185

Shahin, M. Y., 2005. Asphalt Surfaced Airfields: Pavement Condition Index. Funded by U.S. Air Force Civil Engineering Support Agency (AFCESA/CESC), Tyndall Air Force Base, Florida.

Xu, S., Zhang, S., Yang, C., Huang, J., 2020. Development of an Intelligent Pavement System for Real-time Monitoring and Early Warning. *Measurement*, 159, 107797

Yi, L., Zou, L., & Sato, M., 2018. Practical Approach for High-Resolution Airport Pavement Inspection with the Yakumo Multistatic Array Ground-Penetrating Radar System. *Sensors*, *18*(8), 2684.

Yu, J., Li, Y., Ma, C.,, Zhang, R., 2018. A GIS-based Pavement Management System for Airport Runways. In *Proceedings of the 2018 International Conference on Civil Engineering and Materials (ICCEM 2018)* (pp. 200-204).